Upper limits for the existence of long-lived isotopes of roentgenium in natural gold

F. Dellinger, W. Kutschera, O. Forstner, R. Golser, A. Priller, P. Steier, A. Wallner, and G. Winkler
University of Vienna, Faculty of Physics, Vienna Environmental Research Accelerator (VERA) Laboratory, Währinger Strasse 17, A-1090 Wien, Austria
(Received 10 October 2010; published 28 January 2011)

A sensitive search for isotopes of a superheavy element (SHE) in natural gold materials has been performed with accelerator mass spectrometry at the Vienna Environmental Research Accelerator, which is based on a 3-MV tandem accelerator. Because the most likely SHE in gold is roentgenium (Rg, $Z = 111$), the search concentrated on Rg isotopes. Two different mass regions were explored: (i) For the neutron-deficient isotopes ^{261}Rg and ^{265}Rg, abundance limits in gold of 3×10^{-16} were reached (no events observed). This is in stark contrast to the findings of Marinov *et al.* [Int. J. Mod. Phys. E **18**, 621 (2009)], who reported positive identification of these isotopes with inductively coupled plasma sector field mass spectrometry in the $(1 - 10) \times 10^{-10}$ abundance range. (ii) Theoretical models of SHEs predict a region of increased stability around the proton and neutron shell closures of $Z = 114$ and $N = 184$. We therefore investigated eight heavy Rg isotopes, ^{A}Rg, $A = 289$, 290, 291, 292, 293, 294, 295, and 296. For six isotopes no events were observed, setting limits also in the 10^{-16} abundance range. For ^{291}Rg and ^{294}Rg we observed two and nine events, respectively, which results in an abundance in the 10^{-15} range. However, pileup of a particularly strong background in these cases makes a positive identification as Rg isotopes—even after pileup correction—unlikely.

DOI: 10.1103/PhysRevC.83.015801 PACS number(s): 07.77.Ka, 07.77.Gx, 32.10.Bi, 82.80.Rt

I. INTRODUCTION

Calculating the stability of heavy nuclei has always been a challenge to nuclear theorists. In the 1960's an exciting possibility emerged when shell-model corrections to the liquid-drop model indicated that there may be a neutron-rich "island of stability" beyond any known nuclide [1–5]. Nucleosynthesis calculations indicated that such nuclei may be produced under stellar *r*-process conditions [6]. For the superheavy nucleus with $Z = 110$ and $N = 184$, a half-life of 2.5 billion years was calculated [5]. A specific search with accelerator mass spectrometry (AMS) for this isotope was therefore performed in 1980 on a platinum nugget [7]. It was assumed that element $Z = 110$ has similar chemical properties to platinum. No events of a ^{294}110 isotope were observed with an abundance limit of $^{294}110/\mathrm{Pt} = 1 \times 10^{-11}$. By assuming a supernova-produced $^{294}110/\mathrm{Pt}$ ratio of 0.02 to 0.06 [6], one can conclude from the observed abundance limit that the half-life must be less than ∼200 million years, provided that element 110 follows platinum throughout the geochemical and geophysical history of the Earth. Many other searches for superheavy elements (SHEs) in natural materials were performed [8,9]. To this day, no confirmed evidence exists for long-lived SHE isotopes in nature, however, recently some evidence has been reported for the occurrence of long-lived neutron-deficient isotopes of thorium [10] and of roentgenium ($Z = 111$) in natural gold [11], and of a SHE ($Z \sim 122$) isotope of mass 292 in thorium [12]. These measurements were performed with high-resolution inductively coupled plasma sector field mass spectrometry (ICP-SFMS). Because it seems difficult to measure the reported abundance levels in the $10^{-10} - 10^{-12}$ range with ICP-SFMS, these extraordinary results certainly need independent verification by other experimental techniques.

So far two searches with AMS were performed: one at the Maier Leibniz Laboratory of the Ludwig-Maximilians-Universität (LMU) and Technische Universität (TU) Munich [13], and another one at the Vienna Environmental Research Accelerator (VERA) Laboratory of the University of Vienna [14]. Both of these AMS searches concentrated on thorium. The work from Munich [13] set upper limits of $\sim 1 \times 10^{-12}$ for the abundance of neutron-deficient thorium isotopes (^{211,213,217,218}Th) relative to ^{232}Th, while the work in Vienna [14] lowered these limits to $\sim 5 \times 10^{-15}$. Thus the abundances of $(1 - 10) \times 10^{-11}$ for these isotopes reported by Marinov *et al.* [10] were not confirmed. In addition, a SHE nuclide with mass-292 observed by Marinov *et al.* [12], with an abundance of $\sim 1 \times 10^{-12}$ in ^{232}Th, was not seen in the work performed in Vienna [14] with an upper limit of 4×10^{-15}.

Figure 1 shows a schematic presentation of the AMS facility in Vienna, indicating the setup for measuring ultralow abundances of long-lived nuclides in natural gold samples. As compared to ICP-SFMS, which essentially identifies the claimed SHE isotopes only through high-resolution mass measurements, the AMS setup at VERA utilizes a system that eliminates background by a highly redundant filtering process. Clearly this is an advantage for proving the existence of such a rare species once a positive signal is observed. However, it must be pointed out that the complexity of the AMS system requires a very good calibration with known pilot beams (as discussed in Sec. III), in order to be sure that the setup is sensitive to detect SHE nuclides. Simply speaking, it is easier to miss rare species with AMS than with ICP-SFMS. On the other hand, it is very difficult to be sure that events observed with ICP-MS are not caused by an unidentified background.

In the current work we report on AMS measurements of roentgenium (Rg) isotopes in natural gold materials. Similar to the arguments in the early paper on the platinum experiment [7], we assume that Rg ($Z = 111$) chemically follows Au ($Z = 79$). Estimates of relativistic effects on the electron configuration suggest that this assumption may hold [15,16]. The goal of the current work was, on the one hand, to check

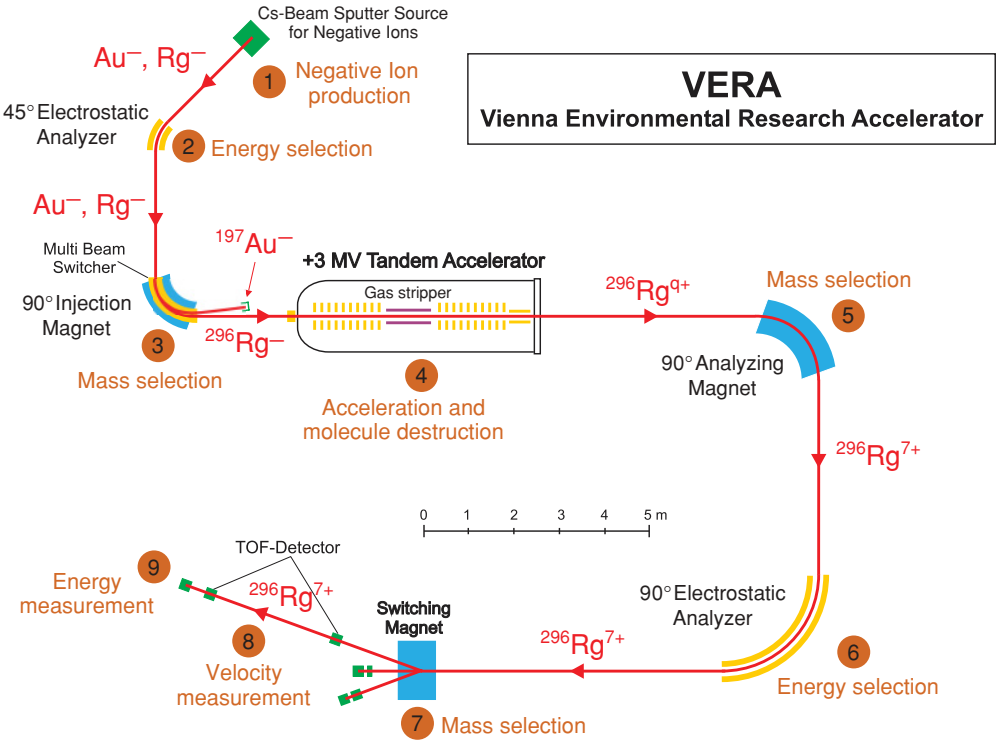

FIG. 1. (Color online) Schematic presentation of the setup for the detection of ^{296}Rg with VERA. The ninefold filtering process used in our highly selective SHE measurements is indicated: (1) negative-ion production (including background ions not indicated in the figure but used partly as reference ions; see text), (2) energy/charge selection, (3) momentum/charge selection (mass sensitive), (4) breakup of molecules in the gas-stripping process, (5) momentum/charge selection, (6) energy/charge selection, (7) momentum/charge selection, (8) TOF (velocity) measurement, (9) residual energy measurement.

the positive reports on the neutron-deficient Rg isotopes, ^{261}Rg and ^{265}Rg [11], and, on the other hand, to extend the search to neutron-rich Rg isotopes, $^{289-296}$Rg, covering the area of increased stability predicted around the magic neutron number $N = 184$, e.g., in Ref. [17].

Strictly speaking, only the measurement of the velocity and the energy with the final two parameters (8 and 9 in Fig. 1) directly determines the atomic number of a superheavy nuclide. The preceding part of the AMS system is sensitive to a selected mass-to-ionic charge (m/q) ratio, within a mass bandwidth of ~0.2 atomic mass units (amu). This bandwidth means that we would also accept SHE isotopes that deviate with their actual mass from the calculated ones [18]. In addition, the finite bandwidth is also advantageous for a search into the unknown, because, owing to the small mass changes along isobars [18], it would also include several isobars around the respective Rg isotope. However, because Rg is the most likely element to follow gold, in our search we refer only to Rg isotopes. Nevertheless, we think it is important to point out that for each Rg isotope we would be able to see superheavy isobars of neighboring elements as well, should they happen to be present in gold in detectable quantities.

In Sec. II the sample materials and the preparation for the AMS measurements are described. In Sec. III we present the tuning procedure of VERA for the detection of SHE isotopes and the setup for AMS measurements in the search for different Rg isotopes. In Sec. IV the results for the ten different Rg isotopes are presented and discussed. Finally, in Sec. V we present a brief conclusion and its consequences for future searches for SHEs in nature.

II. SAMPLE MATERIAL AND PREPARATION

The Periodic Table of Elements arranges elements in groups according to their chemical behavior. Elements of the same group have similar chemical properties. As recent experiments show, this trend seems to hold also for superheavy elements [19–22], however, exceptions of that trend at the beginning of the superactinide series are known (see Ref. [19] and references therein). Theoretical considerations on the influence of relativistic effects on the ordering of the atomic-level scheme predict Rg to be possibly an even nobler metal than gold [15,16], although with a d^9s^2 ground-state configuration instead of the $d^{10}s^1$ configuration found in the other coinage metals: Cu, Ag, and Au. The relativistic calculations [15] also give an electron affinity (EA) of Rg, which is 1.56 eV. This EA lies between the ones for Au (2.31 eV) and Ag (1.30 eV) [23], elements which are known to form prolific negative ions in Cs-beam sputter sources [24]. Both the chemical resemblance to its lighter homologues and the ability to form negative ions are essential prerequisites for the validity of our measurements.

Each step of a chemical preparation procedure holds the risk of unintentionally separating the superheavy atom species

TABLE I. Compilation of the natural samples used in our search for neutron-deficient and superheavy Rg isotopes. The location and the total mass of the samples are listed. Not all of the material was used up in our measurements.

Sample name	Location	Sample mass
VIC-55	Victoria, Australia	636 mg
VIC-50	Victoria, Australia	347 mg
YUK-3–82	Yukon, Alaska, USA	31 mg
NHM-GK	Goldkuppe, Freiwaldau, Silesia, Czech Republic	62 mg
NHM-VER	Verespatak, Romania	19 mg

from (chemically homologous) sample bulk material, if the chemical behavior is only slightly different than what is expected. So the safe way is to omit chemical purification if one is not absolutely sure about the chemistry of the SHE.

Using a highly sensitive measurement technique such as AMS allows the search for SHEs in natural (i.e., chemically unpurified) materials. Compared to other (more simple) measurement techniques, the background in AMS measurements is generally small and most interferences can be identified and/or suppressed (see Sec. IV).

Following the arguments presented above, we consider natural gold as the most promising sample material to search for superheavy Rg species, especially if such materials already lead to the claim of finding "exotic" nuclei [11]. Thus three gold nuggets purchased at a mineral shop on the Internet and two historical gold samples donated by the Department of Mineralogy and Petrography Department of the Natural History Museum, Vienna (NHM) were used as sample materials for this study (see Table I). Furthermore, high-purity gold wire supplied by Goodfellow (sample name GF) was added as a complementary sample type, which underwent chemical pretreatment. Small pieces (a few milligrams) were cut off the samples with a clean knife and pressed into aluminum target holders of our multi-cathode source of negative ions by Cs sputtering (MC-SNICS) Cs-beam sputter source [25,26].

III. TUNING PROCEDURE AND AMS MEASUREMENTS AT VERA

In order to establish reliable setups for the search of SHE isotopes by AMS, it is important to use molecular-ion beams composed of known isotopes, with ion-optical properties as close as possible to the SHE isotopes of interest. A beam of singly charged negative *molecular* ions of nearly the same mass as the rare-ion species is used to tune the low-energy side of the AMS facility, VERA (see Fig. 1). At the tandem terminal gas stripper, operated with oxygen, these molecules break up and isotopes with a close-lying mass-to-charge (m/q) ratio with respect to the searched-for rare-ion species can be used to tune the high-energy side of the AMS facility. Based on an accurately established pilot-beam setup, the setups for the SHE-isotope detection are obtained by scaling the settings of the electric devices only (i.e., multibeam switcher, tandem terminal voltage, 90° electrostatic analyzer, electrostatic steerers) to the appropriate values for SHE detection. All magnetic elements are thereby left unchanged to maintain reproducibility and accuracy of the measurement setups, even when alternating repeatedly between the pilot-beam and SHE-isotope setups. Because no experimental mass values exist for SHEs, the predicted mass values given to a precision of 0.1 amu from Ref. [18] were used to scale for the SHE isotopes.

An important aspect of the accelerator setup for the detection of SHE isotopes is the m/q acceptance, because the calculated SHE masses may deviate from the actual ones by approximately ±0.1 amu. In our previous search for SHE isotopes in natural thorianite [14], this question was addressed in the following way. The long-lived isotope ^{232}Th ($t_{1/2} = 1.4 \times 10^{10} a$) decays via α emission and two consecutive β^- decays into short-lived ^{228}Th ($t_{1/2} = 1.9a$). In secular equilibrium this leads to an isotope ratio of $^{228}\mathrm{Th}/^{232}\mathrm{Th} = 1.36 \times 10^{-10}$. Because the masses of these isotopes and their isotope ratio are accurately known, an AMS measurement was performed by successively scaling the setup for ^{228}Th detection close to the actual mass of ^{228}Th in steps of 0.1 amu. The number of detected ^{228}Th counts, normalized to the $^{232}\mathrm{ThO}_2^-$ current, follows a Gaussian-shaped distribution with $\sigma \sim 0.15$ amu. Therefore we can assume that our AMS setup accepts actual masses of SHE isotopes within a bandwidth of at least 0.2 amu, as compared to the theoretical value [18].

For the tuning materials Te_2 and VTe_2 (a mixture of vanadium powder and tellurium powder in a ratio of 1 : 2), a full scan of isotopologues (identical molecules with different isotopic composition) was performed to assure that the correct mass peak is selected (see below).

In the case of the neutron-deficient Rg setups, $^{128,130}\mathrm{Te}_2^-$ ($m = 258$) was used to set up the low-energy side of VERA for $^{261}\mathrm{Rg}^-$ and $^{265}\mathrm{Rg}^-$. After molecule breakup, the atomic fragment $^{130}\mathrm{Te}^{3+}$ was used to tune the high-energy side for $^{261}\mathrm{Rg}^{6+}$ and $^{265}\mathrm{Rg}^{6+}$. In the search for superheavy Rg isotopes, $^{51}\mathrm{V}^{126}\mathrm{Te}_2^-$ ($m = 303$) was utilized to establish the low-energy setup for $^{289-296}\mathrm{Rg}^-$, whereas the fragment $^{126}\mathrm{Te}^{3+}$ allowed to tune the high-energy side for $^{289-296}\mathrm{Rg}^{7+}$.

The less the m/q ratios of the SHE isotope deviate from the m/q ratios of the pilot beam, the more reliable the established setup is for the SHE isotope—although m/q ratios that are too close may cause a strong background for the SHE detection. Previous measurements at VERA with heavy isotopes (see, e.g., Refs. [27] and [28]) proved that settings of the AMS system can be reliably scaled for a 2.5% shift in m/q ratios. In Table II the relative difference of the m/q ratios of the outermost masses in the current study are listed. It is worth mentioning that all m/q ratios of the rare ions lie in near proximity to the values of the pilot ions, where reliable scaling is proved.

One beam time consisted of a large number of runs on different target materials. Within one run, a sequence of various SHE-isotope setups and reference-ion setups—all scaled from the same tuning setup—are measured. At the beginning and at the end of each run a separate setup is loaded to measure the

TABLE II. Comparison of the m/q ratios of SHE ions and the tuning-ion species.

High-energy tuning ion	m/q of tuning ion	SHE ion	m/q of SHE ion	$\Delta(m/q)/(m/q)$ (%)
$^{130}Te^{3+}$	43.33	$^{261}Rg^{6+}$	43.50	0.38
$^{130}Te^{3+}$	43.33	$^{265}Rg^{6+}$	44.17	1.92
$^{126}Te^{3+}$	42.00	$^{289}Rg^{7+}$	41.29	−1.70
$^{126}Te^{3+}$	42.00	$^{296}Rg^{7+}$	42.29	0.68

Au^- current output of the target used for calculating the final atom ratios.

The $^{197}Au^-$ current measured in an off-side Faraday cup on the low-energy side (see Fig. 1) between the individual runs typically ranged from 10 to 40 μA for all measurements. The transmission from the injector (low-energy current) to the detector (registered counts) was estimated to be 1.5×10^{-3} for the measurements of neutron-rich Rg isotopes ($A = 289$–296) and 3×10^{-3} for the measurements of the neutron-deficient Rg isotopes ($A = 261, 265$). The lower charge state selected in the measurements on neutron-deficient Rg isotopes results in a higher stripping probability in the terminal stripping process as compared to the neutron-rich Rg isotopes. Because detector efficiency [Bragg and time-of-flight (TOF) detector] and charge state probability of the stripping process contribute to the main factors, the total efficiency is higher for the neutron-deficient Rg isotopes. The stripping efficiency has been estimated by extrapolation of the measured charge distributions of ^{197}Au and ^{238}U injected into the terminal gas stripper at the same velocity as the corresponding SHE isotopes.

Most of the measurement time was spent in the SHE-isotope setups (∼200 s per setup and run) and only ∼20 s in the reference-ion setups. The latter were used to monitor the stability of the measurement setup with time. The tuning setup was therefore scaled for ions with close-lying magnetic rigidity (e.g., $^{208}Pb^{5+}$ for $^{293}Rg^{7+}$; Fig. 3) to produce an acceptable count rate of ∼100 Hz in the detection system. If some settings of the AMS-system components would drift with time, these reference count rates would change noticeably.

At the detection system the pulse height and pulse width of signals of a Bragg-type ionization chamber were recorded. Additionally, the TOF signals of a 2.8-m-long TOF section were collected. The combination of these three parameters enabled one to effectively identify pileup events (see Sec. IV).

IV. RESULTS AND DISCUSSIONS

Figure 2 shows the location of the Rg isotopes investigated in the present work in the upper end of the chart of nuclides. We first investigated the neutron-rich Rg isotopes. The search for heavy Rg species in the mass range of 289–296 amu was performed in three separate beam times. In the first beam time on April 6–7, 2009, a total of 33 runs were performed on the targets GF, YUK-3-82, VIC-50, VIC-55, NHM-GK, and NHM-VER to search for $^{293-296}Rg$. A single run consisted of a sequence of measurements in the following order: Au^-

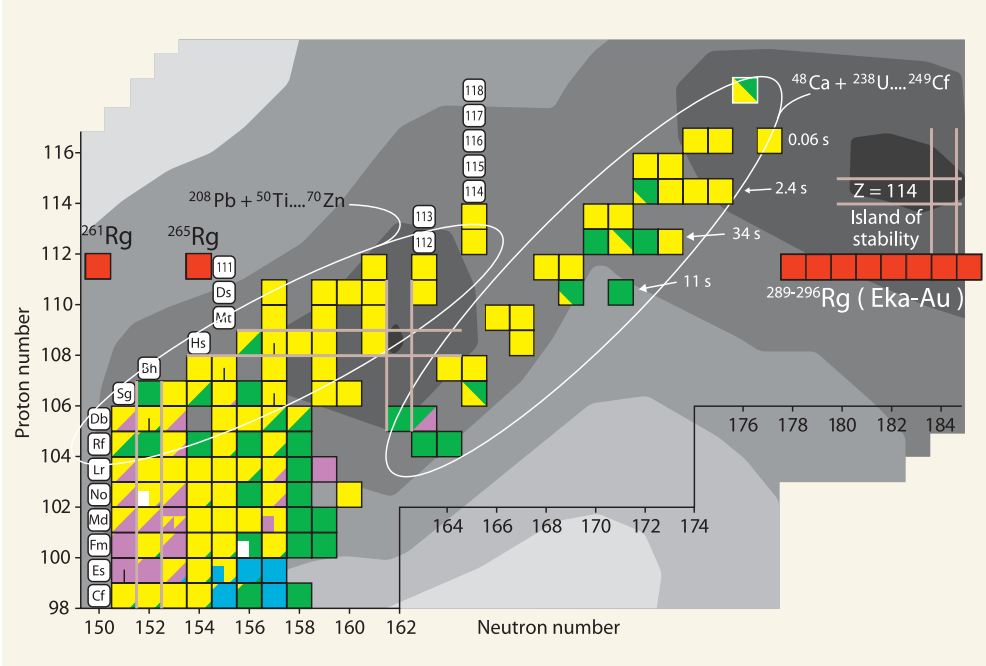

FIG. 2. (Color online) The upper end of the chart of nuclides, as shown in Ref. [29]. The various shades of gray indicate the calculated surface of the stability of nuclides (darker means more stable). The labels on the ellipses indicate the types of heavy-ion reactions that were used to produce the enclosed nuclides. We modified slightly the figure to include the Rg isotopes (red boxes) searched for in our study. As mentioned in Sec. I, the AMS setup would be sensitive also to isobars of neighboring elements not indicated separately in the figure. Whereas the isotopes $^{289-296}Rg$ lie in the close vicinity of the predicted "island of stability," the two neutron-deficient isotopes ^{261}Rg and ^{265}Rg are situated off the region of enhanced stability.

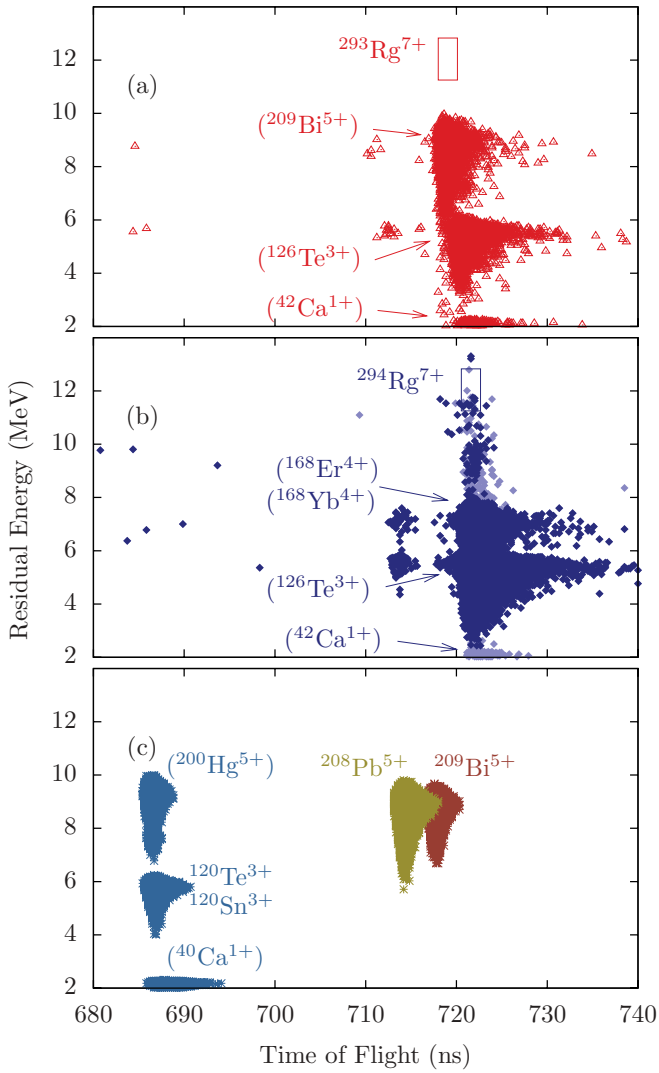

FIG. 3. (Color online) Spectra of residual energy (E_{res}) vs TOF accumulated in the first beam time with the AMS system tuned for the detection of (a) $^{293}Rg^{7+}$ and (b) $^{294}Rg^{7+}$. In (c) the individual spectra of the three reference ions ($^{120}Te^{3+}$, $^{208}Pb^{5+}$, and $^{209}Bi^{5+}$) are plotted together (composite spectrum). To show clearly the peak position of the reference ions, only channels that contain more than ten events are plotted in spectrum (c). In contrast, all events are shown in (a) and (b). Whereas not one single event was detected in the expected area for $^{293}Rg^{7+}$, several events were detected at the lower end of the window for $^{294}Rg^{7+}$. Most probably those events stem from pileup events of two $^{126}Te^{3+}$ ions reaching the detection system almost simultaneously. When the pulse-width criterion (see Fig. 7) is applied, some events can be rejected (light blue), although eight events still remain within the window. Isotope labels in brackets indicate the possible assignment of ions based on the TOF and residual energy signals for all three plots.

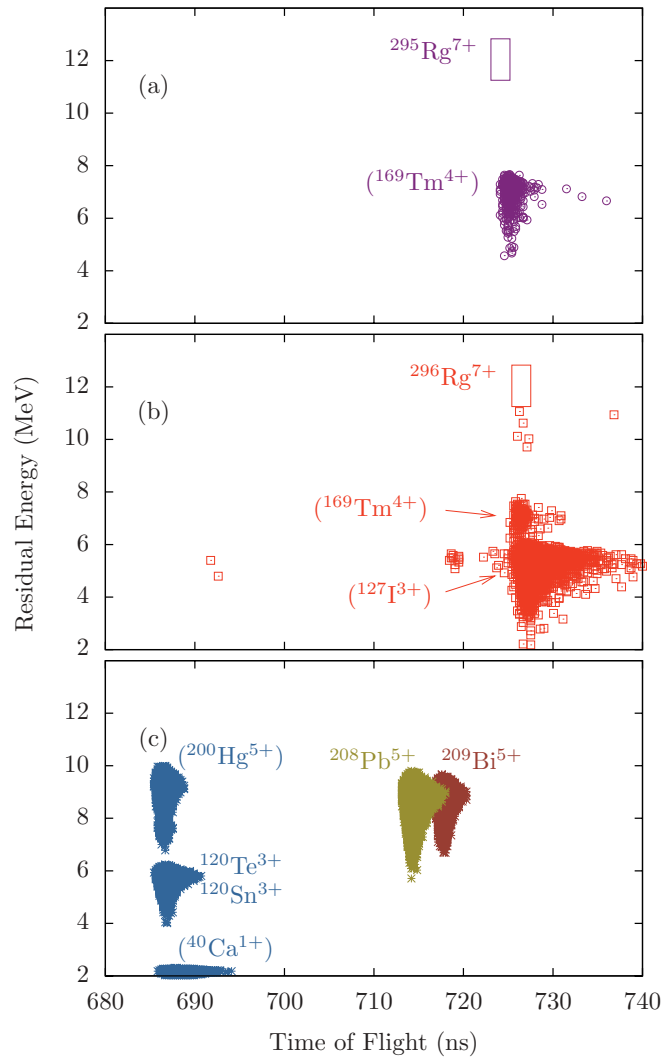

FIG. 4. (Color online) E_{res} vs TOF spectra for (a) $^{295}Rg^{7+}$, (b) $^{296}Rg^{7+}$, and (c) reference ions, plotted in the same way as described in Fig. 3. No events were observed within the Rg isotope windows. Owing to a moderate background in these runs, no pileup events show up.

(∼20 s)–reference ion 1 (∼20 s)–reference ion 2 (∼20 s)–reference ion 3 (∼20 s)–Rg isotope 1 (∼200 s)–Rg isotope 2 (∼200 s)–Rg isotope 3 (∼200 s)–Rg isotope 4 (∼200 s)–Au^- (∼20 s). Including the switching time for setups, this adds up to a total of ∼1000 s per run. The TOF versus residual energy (E_{res}, i.e., the energy after passing the TOF pickup foils and the Bragg detector entrance foils) spectra of all runs of the first beam time are shown in Figs. 3 and 4. There was no event detected within the windows for ^{293}Rg, ^{295}Rg, and ^{296}Rg. However, the setup for ^{294}Rg suffered from an intense background of $^{126}Te^{3+}$, $^{168}Er^{4+}$, and $^{42}Ca^{1+}$ (see Fig. 3), which led to strong pileup signals. Although most of the events could be excluded by the pulse-width criterion [light events in Fig. 3(b)], eight events remained [dark events within the $^{294}Rg^{7+}$ window in Fig. 3(b)]. However, the spectra of the setups for ^{295}Rg and ^{296}Rg (Fig. 4) were almost free of pileup events, and not a single count was recorded at positions where SHE isotopes would be expected. In addition, the remaining events in the ^{294}Rg window [Fig. 3(b)] concentrate in the lower part of the window, contrary to what one would expect for real ^{294}Rg events, which should concentrate around the middle to upper half of the window.

The 38 runs (∼200 s per SHE-isotope setup) on $^{289-292}Rg$ of the second beam time were measured on April 7–8, 2009 by using the same target material as in the first beam time. Figure 5 shows the spectra of E_{res} vs TOF for the ^{289}Rg and ^{290}Rg

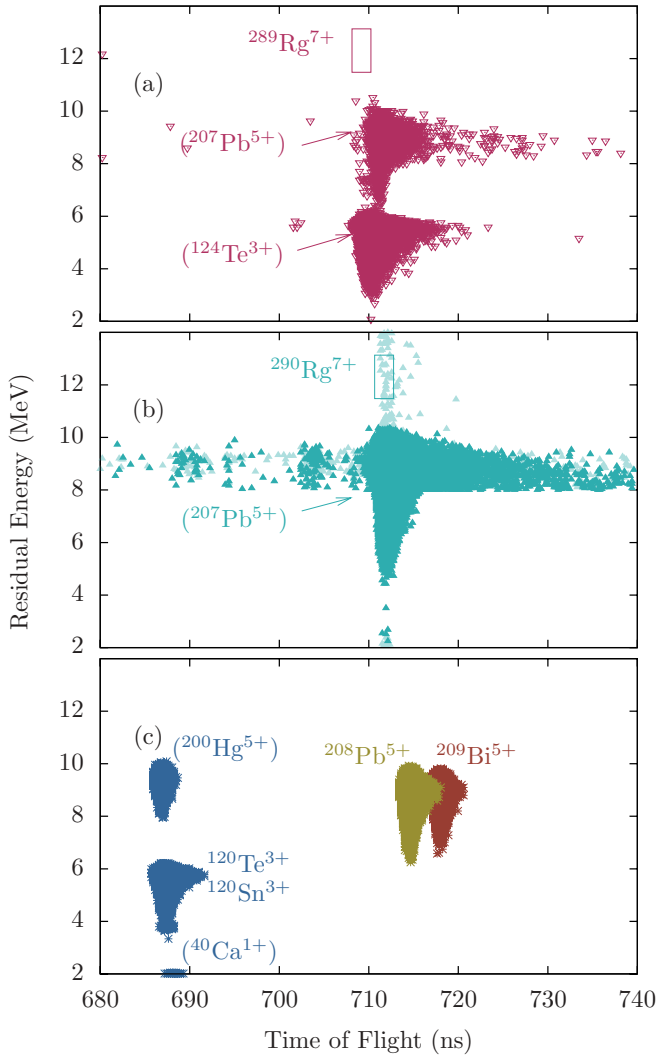

FIG. 5. (Color online) E_{res} vs TOF spectra for (a) ^{289}Rg^{7+}, (b) ^{290}Rg^{7+}, and (c) reference ions, plotted in the same way as described in Fig. 3. These spectra were measured in the second beam time (see text). While the ^{289}Rg^{7+} window is clear from pileup events, the higher background in (b) generates pileup events (light turquoise) in the ^{290}Rg^{7+} window. However, these can all be rejected by the pileup correction (see Fig. 7). To improve the clearness of spectrum (b) below 8 MeV, only channels with more than five events are plotted for this region.

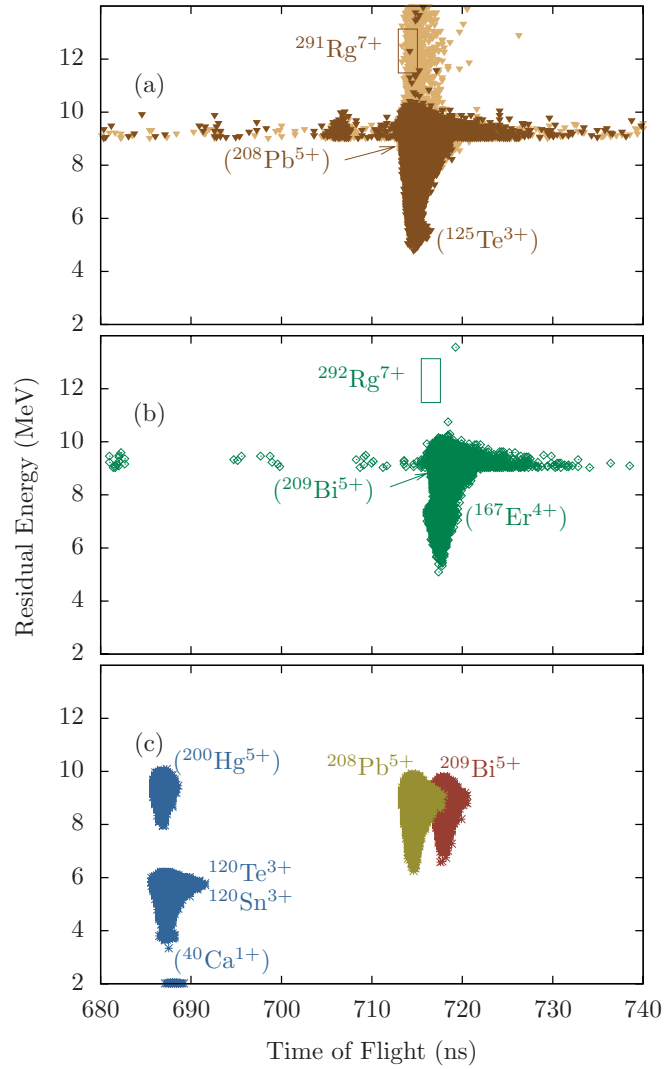

FIG. 6. (Color online) E_{res} vs ToF spectra for (a) ^{291}Rg^{7+}, (b) ^{292}Rg^{7+}, and (c) reference ions, plotted in the same way as described in Fig. 3. These spectra were measured in the second beam time (see text). The ^{291}Rg^{7+} window is covered by an intense belt of pileup events, which could be rejected almost completely by the pulse-width criterion (light brown events). One single event withstood this test. However, because it was surrounded by a large amount of background, it is considered to be uncertain. The ^{292}Rg^{7+} window in contrast is free from pileup. For clearness of spectra (a) and (b) below 9 MeV, only channels containing more than ten events are plotted.

setups. Although the ^{207}Pb^{5+} background reaches the detector with a count rate that is insufficient for pileup creation in the ^{289}Rg setup, it exceeds this level in the ^{290}Rg setup. However, all pileup events in the ^{290}Rg setup can be rejected clearly owing to their pulse-width signal (light turquoise symbols in Fig. 5). In the ^{291}Rg setup (see Fig. 6) an intense belt of ^{208}Pb^{5+} pileup events covering the window for the superheavy ion species can be reduced to one single count in the same way. In both setups the pileup background stems from intense peaks of 5+ ion species.

In Fig. 7 the pileup suppression criterion is illustrated in the case of the setup for ^{291}Rg^{7+}. The efficient pileup identification for 5+ background ions can be shown with the help of the two extreme cases: In the first case, when two 5+ ions reach the detection system at exactly the same time (peak coincidence), E_{res} ($\sim 2 \times 9$ MeV) must differ significantly from the expected value of a detected 7+ ion ($\sim$12.5 MeV). In the second case, when the two pulses of the Bragg-type ionization chamber are slightly shifted in time against each other, leading to a sum pulse height of $\sim$12.5 MeV, their pulse width increases significantly. The first case is situated at the right-hand end of the spectrum in Fig. 7(a), and the latter is situated in the middle of the back-bending pileup belt of Fig. 7(a).

The shape of the region of regular pulses is fitted by a logarithmic function [solid line in Fig. 7(a)] and the distance to that fit is calculated for each event. Events with a distance of

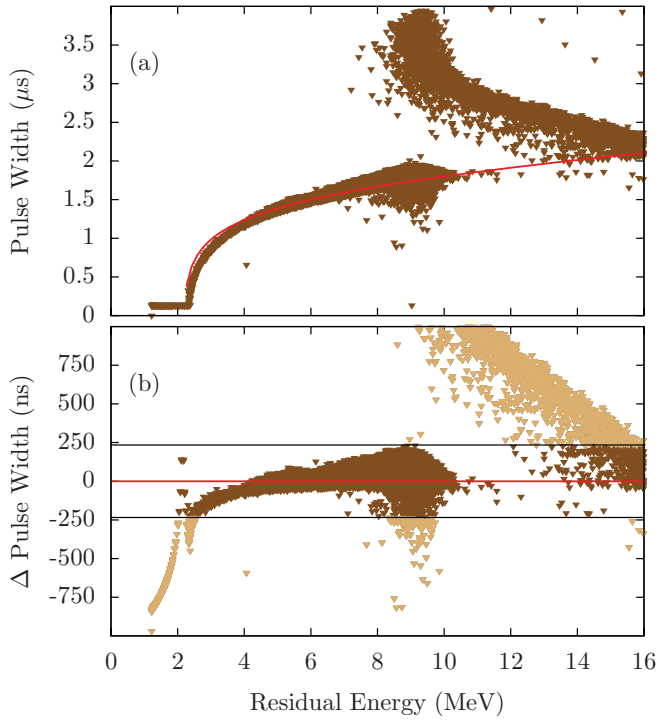

FIG. 7. (Color online) Visualization of the pileup suppression criterion. In (a) the spectrum of pulse width vs residual energy of the setup for $^{291}Rg^{7+}$ is shown. The pulse width is measured after the shaping amplifier at a fixed voltage level corresponding to 2.5 MeV. The narrow belt of regular pulses starts at the lower left-hand side and reduces its slope with increasing residual energy. At the right-hand end of the spectrum, the back-bending belt of the pileup signal starts moving to the upper end of the plot. The solid (red) line indicates a fit function to the region of regular pulses. In (b) the difference of the pulse width of the detected events in (a) to the fit function is plotted. Events that differ more than 235 ns from the curve are not accepted as real events.

more than 235 ns are identified as pileup events [light brown symbols in Fig. 7(b)].

In the setup for ^{292}Rg no event was found within the window of the rare ion. A background of $^{209}Bi^{5+}$ and $^{167}Er^{4+}$ ions was detected at moderate count rates that were too low for pileup production (Fig. 6).

In the last beam time on neutron-rich Rg isotopes on August 15–16, 2009 (38 runs, ∼160 s per SHE setup), the

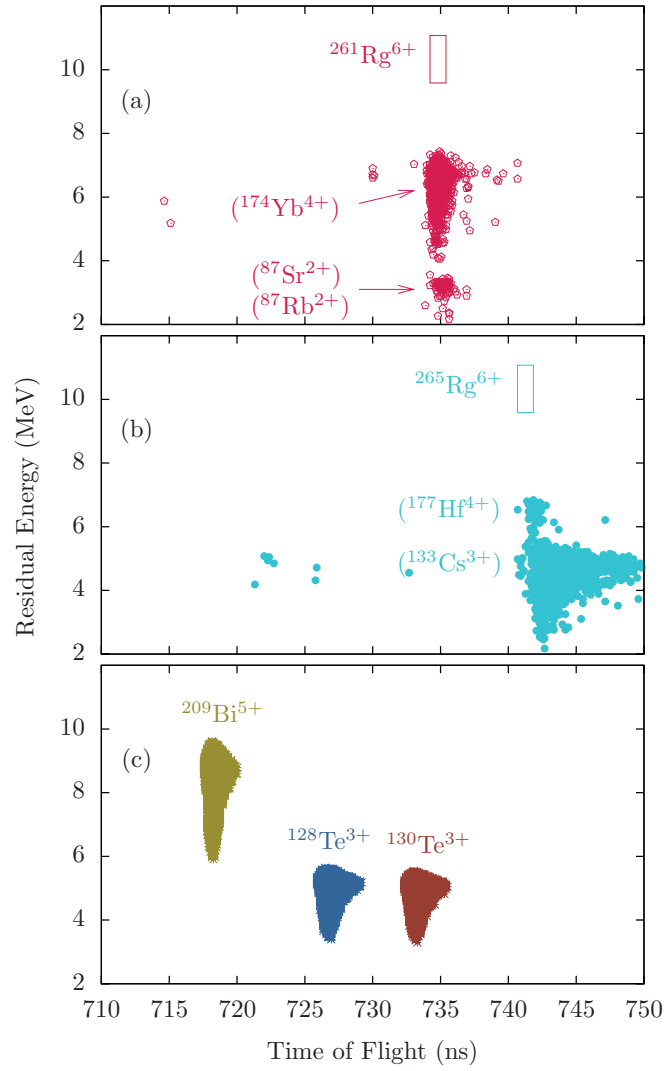

FIG. 8. (Color online) E_{res} vs ToF spectra for (a) $^{261}Rg^{6+}$, (b) $^{265}Rg^{6+}$, and (c) reference ions, plotted in the same way as described in Fig. 3. These spectra were measured in the first beam time on neutron-deficient Rg isotopes (see text). No events were detected in the SHE windows. Two extensively sputtered cathodes were excluded from (b), because they suffered from an atypical high background of $^{133}Cs^{3+}$, most probably from accumulated Cs on the target.

TABLE III. Results of the AMS measurements of neutron-rich Rg isotopes.

Rare isotope	Events detected	Net counting time (hours)	Accumulated $^{197}Au^{-}$ charge(mC)	Abundance relative to ^{197}Au
^{289}Rg	0	2.01	329	$<7 \times 10^{-16}$
^{290}Rg	0	2.01	329	$<7 \times 10^{-16}$
^{291}Rg	2	1.97	139	$(3 \times 10^{-16} - 3 \times 10^{-15})$
^{292}Rg	0	3.47	414	$<5 \times 10^{-16}$
^{293}Rg	0	3.22	411	$<5 \times 10^{-16}$
^{294}Rg	9	3.17	404	$(1 \times 10^{-15} - 4 \times 10^{-15})$
^{295}Rg	0	3.22	411	$<5 \times 10^{-16}$
^{296}Rg	0	3.22	411	$<5 \times 10^{-16}$

TABLE IV. Results of the measurements on the neutron-deficient Rg isotopes.

Rare isotope	Events detected	Net counting time(h)	Accumulated $^{197}Au^-$ charge(mC)	Abundance relative to ^{197}Au		Events expected[a]
				AMS results	ICP-SFMS results [11]	
^{261}Rg	0	6.8	748	$<3 \times 10^{-16}$	$(1-10) \times 10^{-10}$	$7 \times 10^5 - 7 \times 10^6$
^{265}Rg	0	6.2	734	$<3 \times 10^{-16}$	$(1-10) \times 10^{-10}$	$7 \times 10^5 - 7 \times 10^6$

[a]Rare isotope events if abundances of column 6 [11] are assumed.

six isotopes $^{291-296}Rg$ lying near the predicted closed neutron shell ($N = 186$) were remeasured on the targets GF, YUK-3-82, VIC-50, VIC-55, and NHM-GK by using an alternative tuning molecule ($^{27}Al^{126,130}Te_2^-$, $m = 283$). The spectra generally reproduce those of Fig. 3, 4 and 6, however, the background was slightly lower. One count was detected in the lower part of the $^{294}Rg^{7+}$ window and one event remained after suppression of the $^{208}Pb^{5+}$ pileup within the window for $^{291}Rg^{7+}$. The results of the first three beam times are summarized in Table III. In the calculation of the 90% confidence intervals of Tables III and IV, we considered the probability of detecting zero events in a Poisson process given a small rate parameter [30].

The second aim of our study was to test if the claimed findings of Marinov *et al*. [11] could be reproduced at VERA. The first beam time on neutron-deficient Rg isotopes (60 runs, ~200 s per SHE-isotope measurement setup) was performed on April 8–9, 2009. The targets GF and YUK-3-82 mounted in the target wheel had been used up earlier in the search for superheavy Rg, so only VIC-50, VIC-55, NHM-GK, and NHM-VER were investigated in these measurements.

The spectra of E_{res} vs TOF of these 60 runs are shown in Fig. 8. As the windows for $^{261}Rg^{6+}$ and $^{265}Rg^{6+}$ were empty, we could not find any evidence for the existence of those neutron-deficient isotope species. The second beam time session on April 9–10, 2009, on the same target materials (71 runs, 186 s per SHE measurement setup), confirmed the results of the first session. In Table IV the results of our measurements on neutron-deficient Rg isotopes ^{261}Rg and ^{265}Rg are listed.

V. CONCLUSION

Our investigation of the existence of SHE isotopes in natural gold established limits in the range of 10^{-16} for the abundance of two neutron-deficient and eight neutron-rich Rg isotopes. To the best of our knowledge, these are the lowest limits measured so far for these isotopes.

As in our study on neutron-deficient thorium isotopes [14], we could not confirm the findings of Marinov *et al*. [11]. Not a single event was detected in our spectra at positions, where the rare-ion species claimed in Ref. [11] would be expected. Assuming the limits given in Ref. [11], ~10^6 events should have been observed in our measurements. This leads us to the conclusion that the events identified as ^{261}Rg and ^{265}Rg via ICP-SFMS [11] probably originated from an unidentified background.

Although no unambiguous signal has been detected, the stringent limits we could set with our AMS search for Rg isotopes encourages us to extend our search for SHE isotopes to other natural materials. We believe that our AMS approach to find very long-lived SHEs in nature is one of the most sensitive methods to experimentally investigate the predicted "island of stability."

ACKNOWLEDGMENTS

We thank Dr. Uwe Kolitsch of the Department of Mineralogy and Petrology of the Natural History Museum, Vienna, for the donation of sample material used in this study. We also acknowledge useful comments from the anonymous referee.

[1] W. D. Myers and W. J. Swiatecki, Nucl. Phys. **81**, 1 (1966).
[2] S. G. Nilsson, J. R. Nix, A. Sobiczewski, Z. Szymanski, S. Wycech, C. Gustafson, and P. Möller, Nucl. Phys. A **115**, 545 (1968).
[3] V. M. Strutinsky, Nucl. Phys. A **122**, 1 (1968).
[4] S. G. Nilsson, C. F. Tang, A. Sobiczewski, Z. Szymanski, S. Wycech, C. Gustafson, I.-L. Lamm, P. Möller, and B. Nilsson, Nucl. Phys. A **131**, 1 (1969).
[5] E. O. Fiset and J. R. Nix, Nucl. Phys. A **193**, 647 (1972).
[6] D. N. Schramm and W. A. Fowler, Nature (London) **231**, 103 (1971).
[7] W. Stephens, J. Klein, and R. Zurmühle, Phys. Rev. C **21**, 1664 (1980).
[8] G. Herrmann, Nature (London) **280**, 543 (1979).
[9] G. N. Flerov and G. M. Ter-Akopian, Rep. Prog. Phys. **46**, 817 (1983).
[10] A. Marinov, I. Rodushkin, Y. Kashiv, L. Halicz, I. Segal, A. Pape, R. V. Gentry, H. W. Miller, D. Kolb, and R. Brandt, Phys. Rev. C **76,** 021303(R) (2007).
[11] A. Marinov, I. Rodushkin, A. Pape, Y. Kashiv, D. Kolb, R. Brandt, R. V. Gentry, H. W. Miller, L. Halicz, and I. Segal, Int. J. Mod. Phys. E **18**, 621 (2009).
[12] A. Marinov, I. Rodushkin, D. Kolb, A. Pape, Y. Kashiv, R. Brandt, R. V. Gentry, and H. W. Miller, Int. J. Mod. Phys. E **19**(1), 131 (2010).
[13] J. Lachner, I. Dillmann, T. Faestermann, G. Korschinek, M. Poutivtsev, and G. Rugel, Phys. Rev. C **78**, 064313 (2008).
[14] F. Dellinger, O. Forstner, R. Golser, W. Kutschera, A. Priller, P. Steier, A. Wallner, and G. Winkler, Nucl. Instrum. Methods B **268**, 1287 (2010).
[15] E. Eliav, U. Kaldor, P. Schwerdtfeger, B. A. Hess, and Y. Ishikawa, Phys. Rev. Lett. **73**, 3203 (1994).

[16] A. Türler, J. Nucl. Radiochem. Sci. **5**(2), R19 (2004).
[17] A. Sobiczewski and K. Pomorski, Prog. Part. Nucl. Phys. **58**, 292 (2007).
[18] S. Liran, A. Marinov, and N. Zeldes, Phys. Rev. C **62**, 047301 (2000).
[19] M. Schädel *et al.*, Nature (London) **388**, 55 (1997).
[20] R. Eichler *et al.*, Nature (London) **407**, 63 (2000).
[21] Ch. Düllmann *et al.*, Nature (London) **418**, 859 (2002).
[22] R. Eichler *et al.*, Nature (London) **447**, 72 (2007).
[23] J. C. Rienstra-Kiracofe, G. S. Tschumper, and H. F. Schaefer III, Chem. Rev. **102**, 231 (2002).
[24] R. Middleton, 1990, "A negative-ion cookbook," University of Pennsylvania [http://www.pelletron.com/cookbook.pdf].
[25] J. A. Ferry, Nucl. Instrum. Methods A **328**, 28 (1993).
[26] J. Southon and G. M. Santos, Nucl. Instrum. Methods B **259**, 88 (2007).
[27] E. Hrnecek, P. Steier, and A. Wallner, Appl. Radiat. Isot. **63**, 633 (2005).
[28] E. Hrnecek, R. Jakopič, A. Wallner, and P. Steier, J. Radioanal. Nucl. Chem. **276**, 789 (2008).
[29] M. Stoyer, Nature (London) **442**, 876 (2006).
[30] G. J. Feldman and R. D. Cousins, Phys. Rev. D **57**, 3873 (1998).